1967

Emittance of uranium oxides

Peter Christian Held
Iowa State University

EMITTANCE OF URANIUM OXIDES

by

Peter Christian Held

A Dissertation Submitted to the
Graduate Faculty in Partial Fulfillment of
The Requirements for the Degree of
DOCTOR OF PHILOSOPHY

Major Subject: Ceramic Engineering

Approved:

Signature was redacted for privacy.

In Charge of Major Work

Signature was redacted for privacy.

Head of Major Department

Signature was redacted for privacy.

Dean of Graduate College

Iowa State University
Of Science and Technology
Ames, Iowa

1967

TABLE OF CONTENTS

	Page
LIST OF SYMBOLS	iii
INTRODUCTION	1
LITERATURE REVIEW	2
Structural Data	2
Kinetic Data	3
Optical Data	3
Relationship Between Optical Properties	6
Emissivity Calculations	7
EQUIPMENT	12
OPERATIONAL THEORY	17
URANIUM OXIDE SAMPLES	28
EXPERIMENTAL	32
RESULTS	37
DISCUSSION	51
CONCLUSIONS	56
LITERATURE CITED	57
ACKNOWLEDGEMENTS	62

LIST OF SYMBOLS

μ - Microns

ρ_o - Surface reflectivity going from a low to a high index

n - Index of refraction

k - Absorption index

nk - Extinction coefficient

a - Absorption coefficient

I - Incident flux

J - Backscattered flux

K' - Special absorption coefficient

S - Special scattering coefficient

l - Length normal to flux

$\epsilon_{h\lambda}$ - Hemispherical spectral emittance

ϵ - Emittance of unspecified denominations

ρ_e - Reflectance at a surface for inbound radiation

ρ_i - Reflectance at a surface for outbound radiation

σ - Optical constant

β - Optical constant

M - Optical constant

N - Optical constant

O - Optical constant

P - Optical constant

LIST OF SYMBOLS (Continued)

ρ_s - Reflectance at an interface of a coating and substrate

P' - Volume fraction of pores

r - Pore radius

D - Sample thickness

e_θ - Radiant flux emitted at an angle θ

e_n - Radiant flux emitted normal to a surface

$\alpha_{h\lambda}$ - Hemispherical spectral absorptance

$\tau_{h\lambda}$ - Hemispherical spectral transmittance

$\rho_{h\lambda}$ - Hemispherical spectral reflectance

$r_{h\lambda}$ - Hemispherical spectral radiant flux reflected by specimen

$e_{h\lambda}$ - Hemispherical spectral radiant flux emitted by specimen

$i_{h\lambda}$ - Hemispherical spectral radiant flux indicent on specimen

k_1 - Furnace constant for viewing optics of specimen

k_2 - Furnace constant for viewing optics of arc

k_3 - Furnace constant for filtering arc radiation

K - Overall furnace constant

$I_{h\lambda}$ - Arc radiation as measured in the furnace

$R_{h\lambda}$ - Reflected radiation as measured in the furnace

$E_{h\lambda}$ - Emitted radiation as measured in the furnace

LIST OF SYMBOLS (Continued)

C_1 - First radiation constant

C_2 - Second radiation constant

T_a - Apparent temperature ^oK

T - True temperature ^oK

G_b - Bulk density not including open pores

INTRODUCTION

Emittance is a property of great importance in the design of refractory materials. To accurately measure the temperature of a body in non-blackbody conditions a correction must be applied to the brightness temperature to determine the true temperature. In addition, the special possibilities of uranium oxides as fuel materials in anticipated uses such as aircraft or spaceship engines requires a knowledge of the radiative properties of the material and hopefully an atomistic basis for these properties. It is felt that the following study will make some contribution to this store of knowledge for present and future uses.

The property measured in this research was the hemispherical spectral emittance of uranium oxides as a function of temperature, porosity, density, and O/U ratio. Wide variations were used in these variables for the double purpose of matching the variables used in forming the oxides and gaining an understanding of the nature of the material.

LITERATURE REVIEW

Belle (1) has reviewed uranium oxides in detail. The author (2) has also reviewed these oxides in an earlier thesis. Thus, the following literature review is limited to the essentials necessary to understand the emittance measurements performed, the theory of emittance, and the possible relationship of the emittance to the nature of uranium oxides.

Structural Data

Uranium oxides are among the most variable of compounds. At low temperatures the stoichiometric material has the CaF_2 structure (3). Extra oxygen can be taken up in the structure with very little distortion of the lattice to O/U ratios of 2.33 and perhaps to 2.50 (4-10). It is generally felt that only the oxygen lattice is defective (9,11-13) but some studies indicate that uranium lattice defects also exist (14, 15). The position of the extra oxygen ions in the lattice has been worked out by Willis (13). He found displacements of the extra oxygen ions of about 1 Å along the [110] and [111] directions from their assumed sites at ½½½,½00,0½0, and 00½ accompanied by vacancies on the normal oxygen lattice.

Kinetic Data

The activation energy for diffusion of oxygen in uranium oxide has been frequently reported (16-20) as about 27 Kcal/mole (1.18 ev.). However, Smith (20) has reported that this value is probably for diffusion of oxygen through the U_3O_7 structure and that the activation energy for taking up oxygen is only about 12.8 Kcal/mole (0.56 ev.). Willis et al. (21) studied the thermal vibrations of oxygen and uranium ions in the dioxide and found them to be much lower than would be expected for melting to occur at vibrational amplitudes equal to the nearest-neighbor separation. They calculated an oxygen ion vibrational amplitude of 0.44 Å at the melting point of the dioxide.

Optical Data

Measurements of emissivity, reflectivity, and transmissivity on uranium oxides in the literature are few and have not been systematically related to density, composition, and temperature. The best known values are those of Claudson (22) who found the emissivity of unpolished specimens to decrease with temperature. Ehlert and Margrave (23) also measured the emissivity of the dioxide. These data are presented in Table 1.

Table 1. Normal spectral emissivity of UO_2

Temperature (°C)	Emissivity
1,047[a]	0.850
1,320	0.798
1,482	0.628
1,522	0.510
1,580	0.417
1,647	0.402
1,682	0.484
1,780	0.446
1,947	0.370
1,800 - 2,100[b]	0.40 for sinters[b]
	0.51 for powders[b]

[a]All figures except those designated "b" are from Claudson (22).

[b]Figures are from Ehlert and Margrave (23).

Jones and Murchison (24) have measured the normal spectral reflectivity of uranium oxide sinters at room temperature as a function of composition and wave length. They found a measurable separation of the reflectivity at the extremes of the visible wave lengths as a function of O/U ratio with little variation around 0.5μ. At 0.65μ the reflectivity varied from about 0.167 to 0.183 for O/U ratios of 2.003 to 2.203. When translated to emissivity values this is a difference of about 2%.

The index of refraction of uranium oxides has been measured rather more often than other optical constants. Ellis

(25) has plotted n versus wave length for fused oxides having an O/U ratio of 1.993. Ackermann et al. (26) have calculated the index and extinction coefficient for thin films by measuring their transmission. Table 2 shows these data (26) along with reflectance as calculated by the classic equation

$$\rho_o = \frac{(n - 1)^2 + (nk)^2}{(n + 1)^2 + (nk)^2} . \qquad (1)$$

Also included are the values of the index of refraction as taken from the graph of Ellis (25).

Table 2. Optical constants

Wavelength[a] mμ	Index of refraction[a]	Index of refraction[b]	Extinction coefficient[a]	Classic reflectance
800	2.29		0.002	0.154
725	2.34		0.002	0.161
650	2.331	2.321	0.0055	0.1597
600	2.42	2.389	0.009	0.172
550	2.48	2.465	0.024	0.173
500	2.52	2.521	0.098	0.190
475	2.50	2.529	0.155	0.194
450	2.58	2.512	0.220	0.214
425	2.53	2.476	0.282	0.220
400		2.433		

[a]From Ackermann et al. (26).

[b]From Ellis (25).

Companion and Winslow (27) measured the diffuse reflectance of powdered uranium oxides of variable composition and

found that the results of Ackermann et al. (26) on thin films applied also to the bulk material. Gruen (28) had earlier found about the same trends in uranium oxides ground up in alkali halides. Bates has measured the absorption spectra of uranium dioxide single and polycrystals (29). His results are most accurate on single crystals in the infrared, but an estimation of the absorption coefficient, a, at 0.65μ can be made as about 3.8×10^2/cm. This implies an extinction coefficient two orders of magnitude greater than that of Ackermann et al. (26). Bates found the absorption coefficient for single crystals to be an order of magnitude smaller than for polycrystals.

Relationship Between Optical Properties

The term emissivity is used to designate the ratio of the amount of radiation emitted by an opaque, optically smooth body, to the amount of radiation emitted by a black body at the same temperature. It is understood that a black body absorbs all radiation incident upon it. In general, the amount of radiation emitted by a body depends upon composition, size, shape, and surface condition so that the value obtained by comparing its radiative output to a black body at the same temperature is called emittance (30, pp. 28-29).

Emittance is also angularly dependent. For a blackbody the radiation emitted goes by the familiar Lambert's cosine law

$$e_\theta = e_n \cos\theta. \qquad (2)$$

By integration of this equation into specific angular distributions (30, pp. 9-13) one finds that the emitted intensity of the radiation falls off as θ increases. The average emitted intensity over a hemisphere is one-half the normal intensity. However, the emittance remains constant for a blackbody.

Polarization of light at the surface for a non-blackbody usually changes the value of the measured emittance (30, pp. 31-33). For metals this correction increases the emittance slightly at angles above about 30°. Just the opposite is true for many metal oxides and carbon. Dielectric materials conform closely to the cosine law out to about 60 to 65° and then fall off rapidly above 75°.

It is hard to judge where uranium oxides fall in this classification so it is well to assume that it behaves like most oxides having hemispherical emittance values about 8% lower than the normal emittance values.

Emissivity Calculations

In the classical case of a harmonic oscillator the reflectivity can be calculated from the index of refraction

and the extinction coefficient. The calculation of emissivity for real materials depends upon knowing the absorption coefficient, scattering coefficient, and reflectivity of the material. In addition, a model of the material is often necessary to explain the changes in these parameters with composition and temperature.

In semiconductors the absorption of energy can often be related to an energy gap. However, uranium dioxide is not a classic semiconductor but corresponds more closely to the hopping or electron transfer model (31-32). There is reasonable agreement among various authors (9,32,33) on the activation energy for the extrinsic (0.2 ev.) and intrinsic (1.5 ev.) activation energy for electrical conductivity in uranium dioxide. These energies are considerably less than the photon energy of about 1.8 ev. where this study was made.

Bates (29) shows 21 absorption peaks between 2.08 ev. (0.6μ) and 0.0833 ev. (15μ) for uranium oxides with a multiple peak near 0.56 ev. which could correspond to the energy of activation for oxygen solution (20). Other peaks reported by Bates (29) could be related to diffusion of oxygen, extrinsic conduction, or intrinsic conduction. There are, however, peaks enough to account for these processes plus several more. The cut off edge for uranium dioxide is roughly in the visible

region and contains several peaks in its fine structure (29). This condition should provide interesting absorptance-emittance data for uranium oxides.

The commonly measured absorption coefficient, a, is usually measured on thin films and is a bulk constant not connected to various components of internally scattered radiation. The absorption index is related to the absorption coefficient by the relation

$$a = 4\pi kn/\lambda \tag{3}$$

In the more precise derivation of the emissivity of a material one starts with an incident flux I and a backscattered flux J, where K' and S are types of absorption and backscattering factors for the radiation. The differential equations for this condition are: (34)

$$dI/dl = -(K'+S)I + SJ \tag{4}$$

$$\text{and} \quad dJ/dl = (K'+S)J + SI. \tag{5}$$

Equations 4 and 5 have been solved for ceramic materials for coatings (35) and solid materials (36). They are respectively

$$\epsilon_{h\lambda} = 1 - \left[\rho_e + (1-\rho_e)(1-\rho_i) \frac{(1-\beta)M\exp(\sigma D) - (1-\beta)O\exp(-\sigma D)}{MN\exp(\sigma D) - OP\exp(-\sigma D)} \right] \tag{6}$$

and

$$\epsilon = 1 - \left[\frac{(1-\rho_i)^2 + 2\beta(1-\rho_i)(\rho_e+\rho_i) - \beta^2(1+\rho_i)(1-\rho_i-2\rho_e)}{(1-\rho_i)^2 + 2\beta(1-\rho_i^2) + \beta^2(1+\rho_i)^2} \right] \tag{7}$$

where $\sigma = [K'(K'+2S)]^{\frac{1}{2}}$ (8)

$$\beta = [K'/(K'+2S)]^{\frac{1}{2}} \quad (9)$$

$$M = (1+\beta) - \rho_s(1-\beta) \quad (10)$$

$$N = (1+\beta) - \rho_i(1-\beta) \quad (11)$$

$$O = (1-\beta) - \rho_s(1+\beta) \quad (12)$$

$$P = (1-\beta) - \rho_i(1+\beta). \quad (13)$$

ρ_e is the reflectance at the surface for inbound radiation

$$\rho_e = \tfrac{1}{2} + \frac{(n-1)(3n-1)}{6(n+1)^2} + \left[\frac{n^2(n^2-1)^2}{(n^2+1)^3}\right] \ln \frac{(n-1)}{(n+1)} - 2n^3 \frac{(n^2+2n-1)}{(n^2+1)(n^4-1)} + \left[\frac{8n^4(n^4+1)}{(n^2+1)(n^4-1)^2}\right] \ln n. \quad (14)$$

ρ_i is the internal reflectance for radiation bound for the surface from inside the body

$$\rho_i = 1 - (1-\rho_e)/n^2. \quad (15)$$

ρ_s is the reflection at the interface between the coating and the substrate and is here assumed to be zero.

Values calculated for these two emissivity expressions are both 0.832 for uranium dioxide using approximate values of $K' = 760/cm$ as approximated from Bates (29), $n = 2.331$ (26), and $S = 75/cm$ as approximated from Folweiler and Mallio (36) from the expression

$$S = 3/4(\text{scattering factor})\ P'/r. \quad (16)$$

The scattering factor varies between zero and four and tends

toward two. P' is the pore fraction, and r is the pore radius (both estimated as lying between the limits of $0.01 < P' < 0.1$ and $100\mu < r < 20\mu$). The emissivity calculated from the classic equation is 0.840.

Thus, the calculated values of emissivity for uranium dioxide agree very well with the experimentally measured values of Jones and Murchison (24). The agreement is so excellent as to suggest that very accurate emittance values for uranium oxides could be calculated if the various optical constants were known as a function of O/U ratio, temperature, and wave length. Unfortunately these values are not known.

EQUIPMENT

The two main components of equipment used in these measurements were an arc imaging furnace and an optical sensing device. The furnace was an Arthur D. Little-Strong product using rare-earth-cored positive electrodes to obtain radiation in the visible wave lengths. Two elliptical mirrors were aligned so that one focal point of each was at the arc and sample while the second focal point of each was at a mutual crossover point where light intensity measurements were made. The first focal points of the mirrors were at the outer plane of the mirrors so that hemispherical viewing was closely approximated. The light flux was picked up with two quartz light pipes which were attached to the same hub and fed through a filtering system into a photocell. The quartz tubes were partially enclosed in stainless steel, bent to shape and coated with epoxy resin in the places where it was difficult to shape the stainless steel to them. The photocell was a Hoffman model 51C barrier type with an output of several hundred millivolts before reaching a saturation value. The light filters consisted of a piece of infrared absorbing glass approximately one centimeter thick combined with the filter from a Leeds and Northrup optical pyrometer (catalogue number 8623). Ten

determinations of the effective wave length of this combination gave a value of 0.656μ with a sample standard deviation of 0.004μ. A second filter combination of a number 70 Wratten filter and the infrared absorbing glass was also used in a few emittance measurements. The effective wave length of this combination was 0.70μ as determined in a single calibration. The output from the photocell was fed to a dual channel Hewlett Packard oscilloscope model 140A where the arc and reflected plus emitted radiation were measured on one channel and the emitted and emitted plus reflected radiation were measured on the other channel at a greater sensitivity.

The light pipes rotated at 3600 rpm and pointed in opposite directions. Synchronized with the light pipes was a shutter rotating at 1800 rpm. The light pipes then "viewed" radiation from the arc, the sample emitted plus reflected radiation, arc radiation, and emitted radiation through each full cycle of the shutter. The main components of this equipment are shown in Figure 1.

This method of measurement has a rather long history of development. Laszlo (37) was among the first to observe that the emitted radiation and the emitted plus reflected radiation from a sample could be separated by suitable shuttering devices in a solar furnace. Comstock (38) developed suitable

Figure 1. Schematic diagram of the experimental equipment

A - Carbon arc
C - Reimaging mirror
M_1 & M_2 - Synchronous motors
G_1 & G_2 - Optical filters
F - Rotating light pipe
E - Rotating shutter
I - Main shutter
J - Circular opening
H - Photoelectric detector
S - Screens

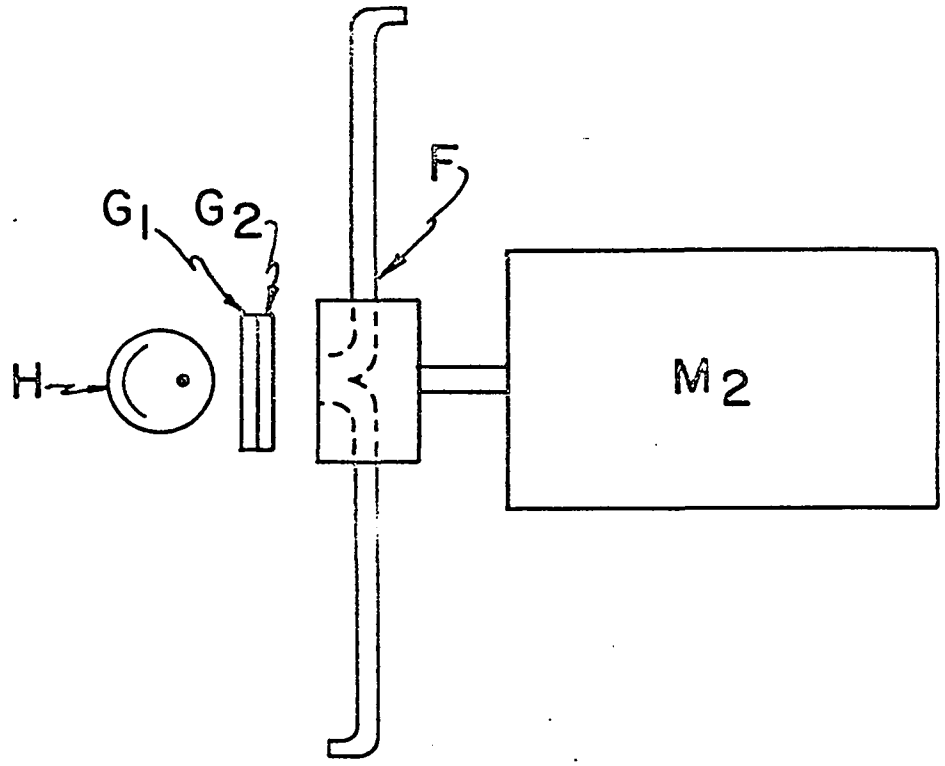
G1
G2
F
H
M2

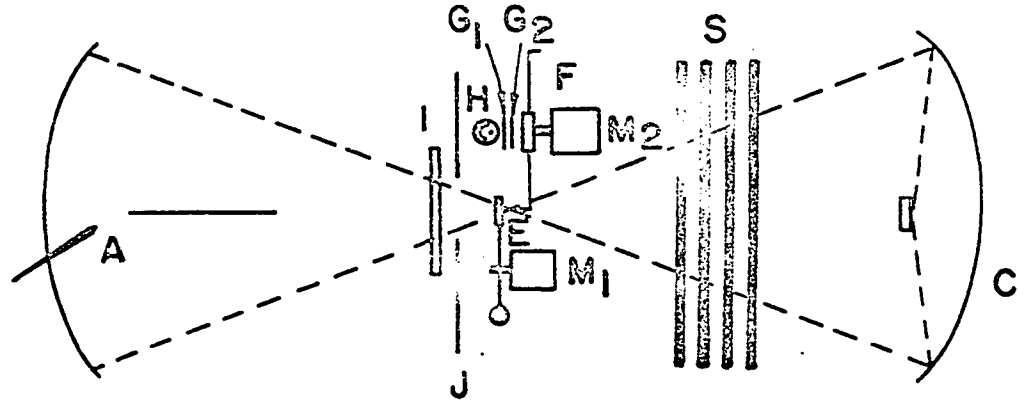
G1
G2
S
F
H
I
M2
A
M1
C
J

adaptations to the arc furnace and made some measurements of emittance. Wilson (39) studied the emittance of space craft materials on equipment very similar to Comstock's. McMahon (40) has made useful adjustments in simplifying the equipment used and in providing dual channel recording which makes the method more sensitive at low temperatures. In fact this is McMahon's equipment except for different filters.

The uranium oxide pellets were heated slowly by inserting four stainless steel screens in the optical path of the furnace. These screens were then removed one at a time after the furnace had been started.

A boron nitride sample holder was used to hold the samples in the focal point of the arc imaging furnace. The holder was contained in a water cooled copper container which also served as a plate to seat the quartz bell jar. The boron nitride was easily cleaned with acetone and showed no signs of volatilization, degradation, or reaction when heated. The quartz bell jars used were evaporating dishes obtained from General Electric. After grinding the top edge to seat on the O ring these jars were 5 cm in diameter by 1.8 cm high. The oxides which deposited on the jar were easily removed with a HNO_3-HCl mixture.

OPERATIONAL THEORY

The hemispherical spectral emittance of the uranium oxide samples was measured from the amplitude of the emitted, emitted plus reflected, and arc radiation in the arc imaging furnace. These amplitudes were given absolute significance when ratios of the same quantities were measured using a primary reflectance as a sample so that an overall furnace constant K was determined.

From the definition of absorptance, reflectance, and transmittance

$$\alpha_{h\lambda} + \rho_{h\lambda} + \tau_{h\lambda} = 1. \tag{17}$$

When the transmittance is zero as was the case here

$$\alpha_{h\lambda} + \rho_{h\lambda} = 1. \tag{18}$$

Further, from Kirchhoff's law as substantiated by Weinstein (41)

$$\epsilon_{h\lambda} = \alpha_{h\lambda}. \tag{19}$$

Then

$$\epsilon_{h\lambda} = \alpha_{h\lambda} = 1 - \rho_{h\lambda} = 1 - r_{h\lambda}/i_{h\lambda}$$

$$= 1 - \left[\frac{(r_{h\lambda} + e_{h\lambda}) - e_{h\lambda}}{i_{h\lambda}} \right]. \tag{20}$$

The output of the photocell can be related to the radiant flux from the sample and arc by the expressions

$$r_{h\lambda} = k_1 R_{h\lambda} \tag{21}$$

$$r_{h\lambda} + e_{h\lambda} = k_1 (R_{h\lambda} + E_{h\lambda}) \tag{22}$$

$$i_{h\lambda} = k_2 k_3 I_{h\lambda} \tag{23}$$

where k_2 and k_3 are viewing optic and pyrometer corrections for the arc radiation and k_1 is a viewing optic term for the sample. Combining Equations 20 through 23

$$e_{h\lambda} = 1 - \frac{k_1[(E_{h\lambda} + R_{h\lambda}) - E_{h\lambda}]}{k_2 k_3 I_{h\lambda}} = 1 - K\left[\frac{(E_{h\lambda} + R_{h\lambda}) - E_{h\lambda}}{I_{h\lambda}}\right] \tag{24}$$

$$= 1 - K\, R_{h\lambda}/I_{h\lambda}. \tag{25}$$

To determine the overall furnace constant K a water cooled brass block of the same size and shape as the sample was polished and coated with several layers of MgO (42). This coating is reported to have a reflectance of 0.972 at 0.65μ (43). Then

$$K = 0.972\ I_{h\lambda}/R_{h\lambda}. \tag{26}$$

A brightness temperature for the sample was obtained by calibrating the output of the photocell against a bulb calibrated by the Bureau of Standards. This process was carried out in three stages. First an optical pyrometer (Pyro, Micro Optical Pyrometer) was calibrated for true temperatures against a bulb calibrated by the Bureau of Standards. The pyrometer was then calibrated against a laboratory bulb

(Westinghouse CPR 6 volts 18 amperes) at set input voltages. Finally the output of the photocell was calibrated against the laboratory bulb at the same input voltages.

Quantitatively, if the output of the photocell is linear

$$e_{h\lambda} = k_1 E_{h\lambda}. \tag{27}$$

The radiant emitted flux is given by Wien's law

$$e_{h\lambda} = C_1 \lambda^{-5} / \exp(C_2/\lambda T_a). \tag{28}$$

Wien's law is an approximation of the more precise Plank's law but introduces less than 0.01% error at short wave lengths (30, p 17). Combining Equations 27 and 28

$$E_{h\lambda} = (1/k_1) C_1 \lambda^{-5} / \exp(C_2/\lambda T_a) \tag{29}$$

$$\ln E_{h\lambda} = \text{constant} - (C_2/\lambda)(1/T_a). \tag{30}$$

The brightness temperature of the sample, T_a, was converted to the true temperature of the calibrated laboratory bulb from the relationship between their radiant emission at the same amplitude

$$e_{Lh\lambda} = C_1 \lambda^{-5} / \exp(C_2/\lambda T) = e_{Sh\lambda} = C_1 \lambda^{-5} e_{h\lambda} / \exp(C_2/\lambda T_a). \tag{31}$$

Equation 31 reduces to

$$T = \frac{T_a}{1 - T_a(\lambda/C_2) \ln(\epsilon_{h\lambda})} \tag{32}$$

A slide rule was constructed to solve Equation 32.

A polaroid of the reflected and arc radiation from a MgO specimen is shown in Figure 2. The overall furnace constant K as determined from these calibrations was found to be between 0.6 and 0.8. A plot of the output from the calibrated laboratory bulb against the reciprocal temperature is shown in Figure 3.

In addition to the theoretical calibrations described above the operation involved here required the use of several other calibration procedures. First there was the problem of calibrating for the quartz bell jar. This calibration was accomplished by setting voltage inputs to a second laboratory lamp (G.E. #49 6 volts) in the same geometric configuration as the sample. The oscilloscope output was measured with and without the bell jar in place at several measured voltages. A single valued correction factor was thus obtained for the absorptance of the bell jar. Emittance measurements were made with four, one, and zero temperature controlling screens in the optical path so calibrations for each of the screen settings was also necessary. This was accomplished in the same manner as for the bell jar. Finally, since uranium oxides have high vapor pressures and deposit an oxide layer on the bell jar, this layer had to be calibrated after each

Figure 2. Typical furnace calibration trace to determine K

Upper level is reflected radiation ($R_{h\lambda}$)

Lower level is arc radiation ($I_{h\lambda}$)

Both versus time (0.5 cm/sec.)

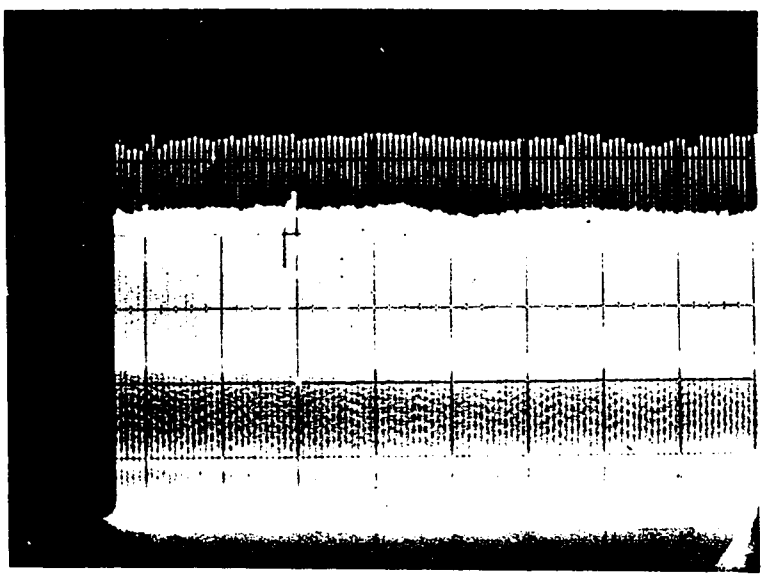

Figure 3. Typical temperature calibration curve showing linearity of photocell and effective wave length of filter

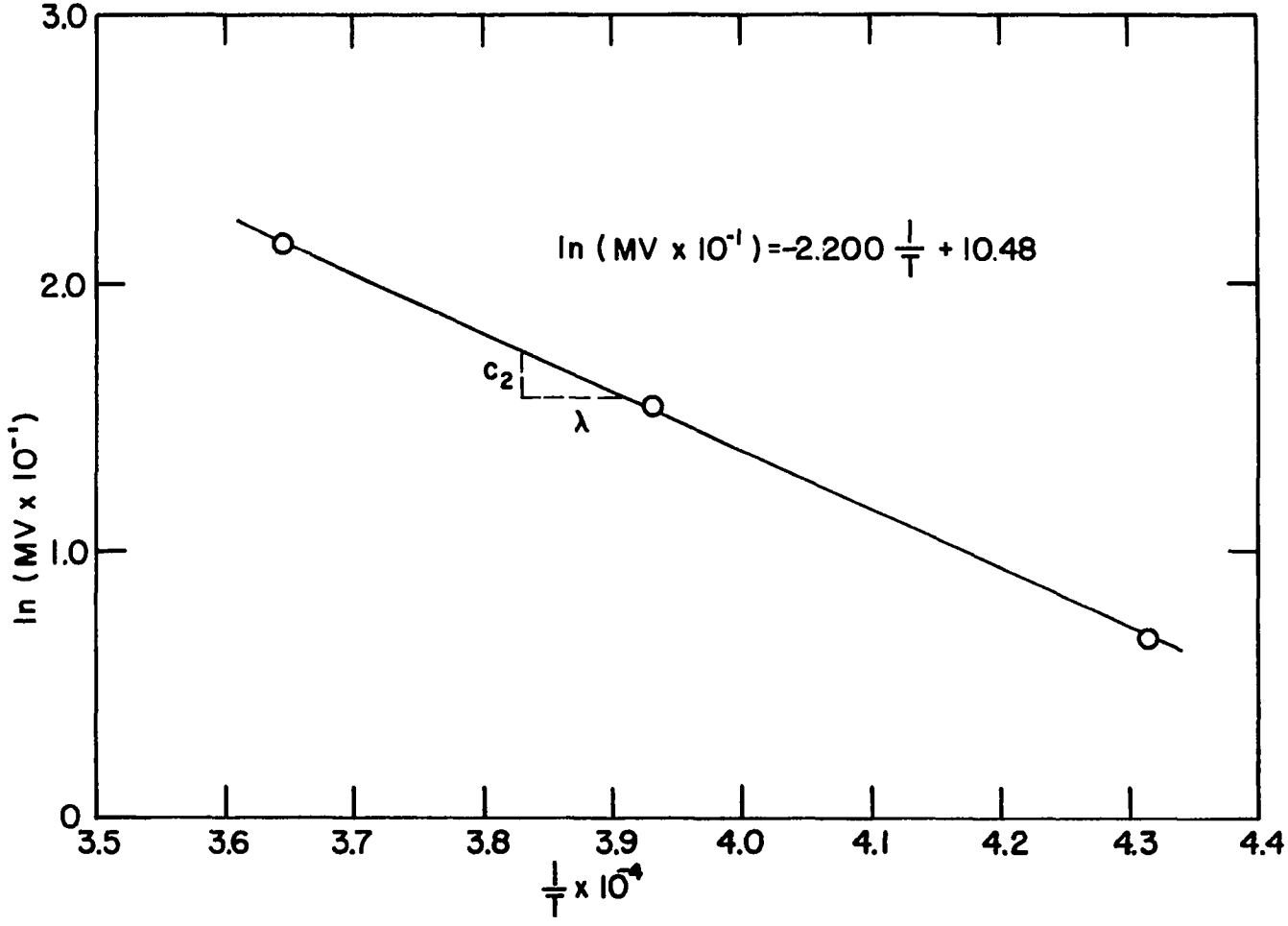
3.0
2.0
1.0
0
ln (MV x 10⁻¹)
ln (MV x 10⁻¹) = -2.200 1/T + 10.48
C2
λ
3.5
3.6
3.7
3.8
3.9
4.0
4.1
4.2
4.3
4.4
1/T x 10⁻⁴

heating. Single valued numbers were also taken for this correction, obtained as with the bell jar, but this factor was weighted as to the time that the furnace was in operation. All measurements were adjusted back to air values as it was impossible to place the bell jar over the laboratory bulb used in the temperature measurements. Figure 4 shows one of these calibrations.

Figure 4. Typical calibration curve for decreased transmission of bell jar, oxide coating, or screens. In this case the oxide coating for sample 1-16

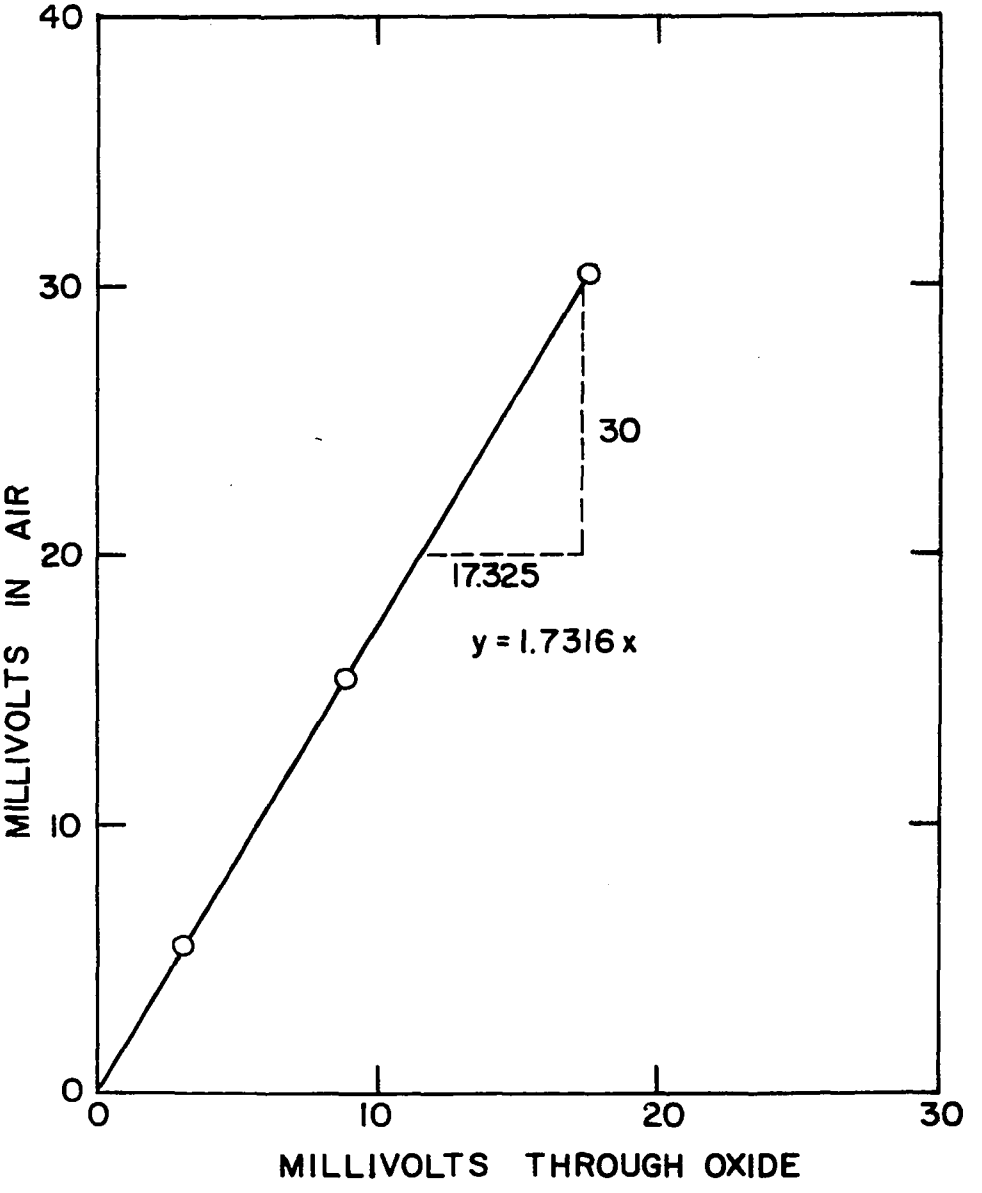
40
30
20
10
0
0
10
20
30
MILLIVOLTS IN AIR
MILLIVOLTS THROUGH OXIDE
30
17.325
y = 1.7316 x

URANIUM OXIDE SAMPLES

The sintering of the samples followed loosely the work of Fuhrman *et al.* (44). It has long been recognized that particles with large surface areas will sinter quite well, and it is also known that uranium oxides with an O/U ratio greater than 2.00 will sinter well. Fuhrman *et al.* (44) broke down agglomerates by oxidizing commercial powders in air at 500°C for one hour which produced the orthorhombic U_3O_8 structure and broke up agglomerates in the process. The powders were then reduced to UO_2 in hydrogen and reoxidized to U_3O_7 to produce a highly defective structure for sintering. The pellets were then reduced to any desired O/U ratio after sintering at 1100°C. They found that commercial powders are quite variable, and in some cases it was only necessary to oxidize the powders to U_3O_7 to produce good quality pellets. In other powders repeated oxidation-reduction steps were necessary to produce good pellets.

Since a variety of pellet densities, stoichiometries, and porosities was desired for this study the simplest technique was attempted first. Mallinckrodt uranium oxide containing 25 ppm iron and not more than 10 ppm of any other metallic impurity was oxidized in air for varying times at

135°C. The powders so obtained were pressed into pellets in a tungsten carbide die at 45,000 psi. These pellets were sintered in a molybdenum resistance furnace under about half an atmosphere of helium for four hours at temperatures from 1300° to 2000°C. Bulk densities and apparent porosities were determined by water immersion. The densities ranges from about 7.5 to 9.7 g/cm^3. O/U ratios were determined on small chips knocked from the bottom of the pellets by oxidation to U_3O_8 in a microbalance at 800°C. It was felt that these samples were useful but that higher density pellets would also be needed. Twenty pellets were produced in this manner and are designated at 1-1 through 1-20 in this report.

A second patch of powder was oxidized to U_3O_8 and then reduced to UO_2 in flowing hydrogen. This process was done twice. An additional oxidation to U_3O_7 was carried out and the samples were then pressed. It was apparent that the particle size of the powder had been reduced as the samples could not be removed from the tungsten carbide die without cracking when pressed to high pressures. By reducing the pressure to 2,700 psi the pellets held together. They were isostatically pressed to 50,000 psi. All of these samples were sintered in slowly flowing nitrogen for four hours at 1200°C. The

densities of these samples were all near 10 g/cm^3 with porosities less than 1%. Two of these pellets were used in this condition, two were further reduced in flowing hydrogen for one half an hour at 1000°C, and two reduced one hour at 1150°C. Two groups of five pellets were resintered at 1300° and 1400°C. One pellet from each five was used without further treatment and two from each group were given each of the above described reduction processes. Sixteen pellets numbered 2-1 through 2-16 were produced in this manner.

It was felt that there were still too few pellets with O/U ratios between 2.1 and 2.2 so a third batch of oxide was prepared and formed using the same techniques as used on the second batch. Initial sintering was carried out at 1400°C and reduction treatments started on pairs of samples at 500°C in flowing hydrogen. The reduction temperature was increased roughly 100°C on pairs of samples with all reduction times being one hour. The reduced pellets were further soaked in flowing nitrogen at 1400°C for four hours to remove possible concentration gradients. Stoichiometry and density were measured as before. The O/U ratio of these samples ranged from 2.19 downward to 2.01 but there were still no specimens in the O/U range 2.10 to 2.16. The fifteen pellets produced in

this series were numbered 3-1 through 3-15.

All of the samples were ground on 600 mesh silicon carbide paper and then polished on a lap with Linde A. The samples were washed carefully after each treatment with distilled water and acetone. A final washing was given each sample with acetone before the emittance measurements were made.

EXPERIMENTAL

The overall constant for the furnace, K, was determined about every day and a half during the measurements, or any time some major change was made in the experimental setup. Emittance measurements were made at low temperatures by substituting a tungsten bulb in place of the arc so that the furnace served only as a geometric unit for measuring emittance. There was some heating of the sample using the tungsten bulb but it was estimated to be below 150°C by considering how hot the samples were when removed from the furnace. Higher temperature measurements were made with four, one, and zero temperature controlling screens in the optical path of the furnace. The measurement made the most often was to start the oscilliscope camera sweep at 0.5 cm/sec with one screen in place and remove this screen during the trace. In this way one could watch the emitted radiation build up, reach a maximum point, and fall off as the coating on the bell jar developed. When a screen was removed from the optical path and the sample was being heated the condition of thermal equilibrium required by Kirchhoff's law was not met. Therefore, emittance values gathered during heating periods are not valid but are included to show qualitatively how rapidly

the material will diffuse energy at these temperatures. Even during fairly stable conditions there was some change in temperature due to coating of the bell jar. It was felt that the emittance values gathered when there was no change in the amplitude of emitted or reflected radiation with time are the most valid, and such values were chosen for the graphs which appear later.

When the O/U ratio of the samples was near 2.0 the samples tended to heat up rapidly upon removal of the last screen. An oxide deposit then collected on the bell jar and the sample cooled slightly. This type of heating is shown in Figure 5. Conversely, when the O/U ratio of the samples was high the oxide coating built up quickly on the bell jar and the increase in temperature on removing the last screen was considerably less. Figure 6 is a polaroid from this type of heating.

The vacuum maintained over the sample presented a considerable problem. If an inert gas atmosphere was maintained it was felt that conductive heat transfer might be large enough to prevent heating or make the radiative transfer of energy not an only effective mechanism, thus throwing off the temperature measurements. Therefore, a partial pressure of

Figure 5. Typical trace from a sample which heats and then cools with oxide layer on the bell jar

Upper curve is emitted plus reflected and emitted radiation ($E_{h\lambda}+R_{h\lambda}$) and ($Eh_{\lambda}$)

Lower curve is arc and emitted plus reflected radiation ($I_{h\lambda}$) and ($E_{h\lambda}+R_{h\lambda}$)
Both versus time (0.5 cm/sec.)

Figure 6. Typical trace from a sample which heats up slowly due to a high vapor pressure of the oxide

Both curves are as in Figure 5

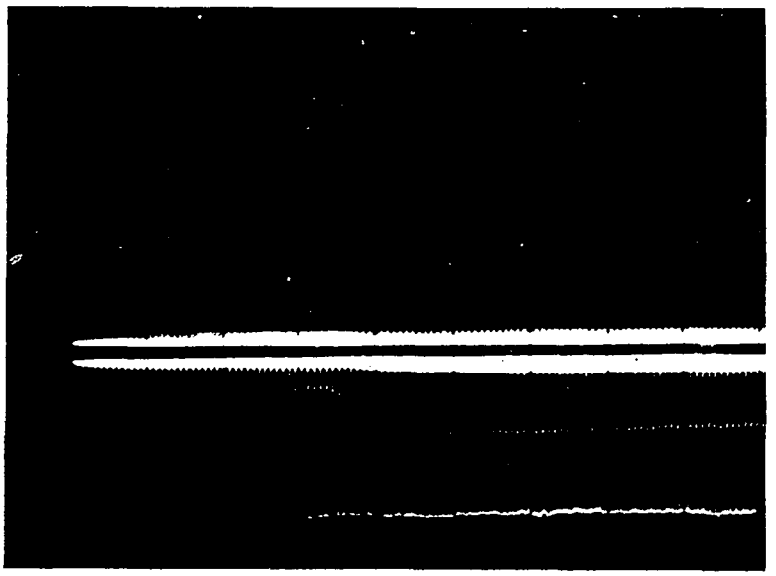

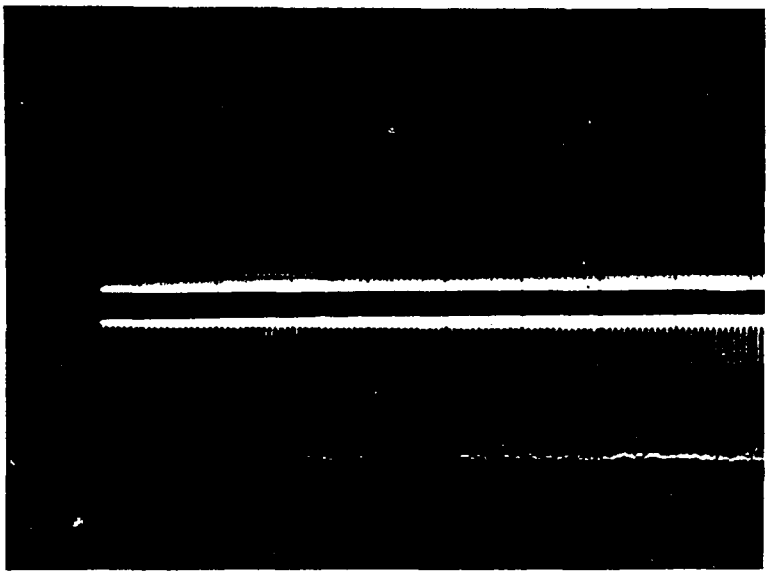

oxygen was maintained over the sample according to the relationship of Aronson and Belle (45)

$$P_{O_2(atm)} = 76[\exp(-3.3\times10^4/T)][\exp(31x/1-x)]$$

where x is the excess oxygen in UO_{2+x}. A temperature of 2200°K was always assumed in the solution of this equation and it was found that a mechanical pump was sufficient to obtain the desired vacuum over the samples. Additional stoichiometry determinations were made on two samples after heating to determine any change in stoichiometry. Sample 2-13 was slightly oxidized from $UO_{2.01}$ to $UO_{2.03}$ while sample 3-8 was reduced from $UO_{2.19}$ to $UO_{2.14}$ during the emittance measurements.

After heating, the samples were allowed to cool for at least half an hour in the water cooled holder. When removed they were not hot to the touch.

RESULTS

The overall description of the pellets and the measured emittances and temperatures are shown in Tables 3 and 4. Plots of emittance versus O/U ratio, for several temperatures and densities are shown in Figures 7 through 10 along with other values shown in the literature. Plots of emittance versus density, temperature, and porosity were not made since examination of Tables 3 and 4 did not show any apparent trends for these variables. The curves drawn through the data points are best line fits. In general these curves have the same trend as the room temperature data of Jones and Murchison (24).

The temperatures and emittances correspond to one another in the following manner. The low temperature emittance was measured at about 450°K, the emittance measured with four screens was taken at about 1000°K, the temperature and emittance with one screen are so labeled as are the maximum temperature and emittance and the end point temperature and emittance.

Table 3. Spectral hemispherical emittance of uranium oxides at 0.656μ

Sample	G_b	O/U ratio	Apparent porosity (%)	$\epsilon_{low\ temp.}$	$\epsilon_{four\ screens}$
1-1	9.948	2.04	16.4	0.78	
1-2	10.412	2.14	10.5	0.71	
1-3	9.859	2.06	15.4	0.79	
1-4	10.221	2.07	16.9	0.79	
1-5	10.455	2.02	12.1	0.76	
1-6	10.364	2.05	7.3	0.73	
1-7	9.808	2.09	18.0	0.80	
1-8	9.562	2.10	19.0	0.80	
1-9	10.071	1.96	10.7	0.74	
1-10	10.326	2.02	10.9	0.78	
1-11	10.412	2.01	10.9	0.76	
1-12	10.299	2.03	9.2	0.75	
1-13	8.378	2.12	7.9	0.82	
1-14	9.332	2.16	5.7	0.83	
1-15	9.227	2.10	16.4	0.83	
1-16	8.275	2.18	4.6	0.82	
1-17	9.524	2.08	17.8	0.82	
1-18	slakes	2.21	--	0.82	
1-19	slakes	2.21	--	0.79	
1-20	slakes	2.24	--	0.83	
2-1	10.019	1.95	0.82	0.70	
2-2	10.023	2.00	0.52	0.75	
2-3	10.017	2.00	0.96	0.72	
2-4	10.024	2.01	0.48	0.70	
2-5	9.965	2.25	0.93	0.68	
2-6	10.186	2.01	0.71	0.78	
2-7	10.192	2.22	0.50	0.72	
2-8	9.946	1.99	0.24	0.70	
2-9	9.185	2.00	0.48	0.75	
2-10	10.026	2.29	0.26	0.71	

$\varepsilon_{one\ screen}$	$\varepsilon_{max.}$	$\varepsilon_{end\ point}$	$\varepsilon_{heat\ up}$	$T_{one\ screen}$	$T_{max.}$	$T_{end\ point}$
0.85		0.85		2002		2095
0.78		0.70		2250		2450
0.80		0.75		2100		2274
0.86		0.80		2024		2213
0.86	0.72	0.77		2102	2320	2274
0.83	0.75	0.75		2094	2318	2288
0.84		0.74	0.72	2086		2283
0.88	0.82	0.84		2153	2384	2325
0.78	0.69	0.70	0.66	2230	2417	2400
0.82		0.75		2221		2400
0.81		0.73		2223		2426
0.77	0.69	0.71	0.64	2287	2482	2428
0.87		0.82		2130		2314
0.83	0.72	0.72	0.70	2317	2530	2530
0.85	0.77	0.82		2290		2388
0.79	0.72	0.74		2052		2444
0.85		0.81	0.79	2035		2198
0.82	0.82	0.83		2285	2367	2306
0.82		0.75	0.78	2249		2442
0.88	0.83	0.85		2118	2277	2215
0.85	0.80	0.84		2153	2275	2214
0.88	0.80	0.80	0.81	2247	2447	2447
0.83	0.75	0.75	0.74	1960	2170	2170
0.79		0.72	0.69	2199		2367
0.84	0.80	0.86		2001	2035	2017
0.81	0.74	0.76	0.72	2228	2304	2350
0.86	0.87	0.91	0.87	low	low	low
0.80	0.73	0.75	0.71	2162	2304	2282
0.79	0.68	0.74	0.65	2245	2449	2415
	0.85	0.88			1997	1951

Table 3. (Continued)

Sample	G_b	O/U ratio	Apparent porosity (%)	$\epsilon_{low\ temp.}$	$\epsilon_{four\ screens}$
2-11	9.972	2.00	0.32	0.72	
2-12	9.911	1.96	0.46	0.73	
2-13	9.988	2.01	0.37	0.71	
2-14	10.157	2.01	0.50	0.72	
2-15	9.978	2.01	0.18	0.73	
2-16	10.047	2.24	0.36	0.71	
3-1	10.318	2.19	3.56	0.71	
3-2	10.458	2.19	5.14	0.75	
3-3	10.407	2.18	4.37	0.73	
3-4	10.518	2.17	0.55	0.68	0.86
3-5	10.542	2.18	0.26	0.71	
3-6	10.307	2.16	3.59	0.73	
3-7	10.654	2.17	0.07	0.69	0.85
3-8	10.574	2.19	10.09	0.73	0.85
3-9	10.166	2.18	3.47	0.71	0.87
3-10	10.385	2.03	0.56	0.69	0.86
3-11	10.392	2.06	0.50	0.73	0.86
3-12	10.101	2.01	4.17	0.74	0.86
3-13	10.109	2.01	3.94	0.75	0.85
3-14	10.398	2.02	0.47	0.68	0.86
3-15	10.344	2.02	10.14	0.71	0.87

$\varepsilon_{one\ screen}$	$\varepsilon_{max.}$	$\varepsilon_{end\ point}$	$\varepsilon_{heat\ up}$	$T_{one\ screen}$	$T_{max.}$	$T_{end\ point}$
0.80	0.72	0.75	0.70	2221	2385	2347
0.78	0.68	0.68	0.64	2232	2471	2455
0.77	0.67	0.74	0.65	2249	2426	2351
0.79		0.72	0.70	2079	2147	2166
0.75	0.64	0.67	0.61	2166	2322	2257
0.92		0.88		low		low
0.88		0.88	0.85	low		low
0.87	0.82	0.88	0.82	low		1918
0.84	0.70	0.82	0.70	1906		1905
0.89			0.68	1820		
0.85		0.86	0.74	2009		1959
0.84		0.83	0.75	1927		1967
0.86		0.86	0.78	1872		1867
0.81		0.77	0.70	1845		1922
0.77		0.65	0.64	1929		2058
0.83		0.76	0.73	1776		1947
0.74		0.70	0.60	1975		1958
0.72	0.57	0.67	0.58	2080	2237	2132
0.78		0.69	0.65	2081		2167
0.76		0.64	0.61	2016		2218
0.73	0.64	0.64	0.60	2078	2240	2240

Table 4. Spectral hemispherical emittance of uranium oxides at 0.70μ

Sample	G_b	O/U ratio	Apparent porosity (%)	ϵfour screens	ϵone screen	ϵmax
2-5	9.965	2.25	0.93	0.91	0.93	0.87
2-14	10.157	2.01	0.50	0.91	0.87	0.85
2-16	10.047	2.24	0.36	0.89	0.95	
3-5	10.542	2.18	0.26	0.91	0.94	
3-8	10.574	2.19	10.09	0.91	0.90	
3-11	10.392	2.06	0.50	0.89	0.88	
3-15	10.344	2.02	10.14	0.90	0.85	

Table 4. (Continued)

Sample	ϵend point	ϵheat up	T_{one} screen	T_{max}	T_{end} point
2-5	0.88	0.87	1935	1990	1985
2-14	0.85	0.79	2002	2111	2111
2-16	0.92	0.93	1891		1920
3-5	0.92	0.92	1937		2000
3-8	0.90	0.85	1931		2055
3-11	0.83	0.81	1959		1962
3-15	0.79	0.75	2110		2245

Figure 7. Emittance of uranium oxides at 0.656μ near room temperature

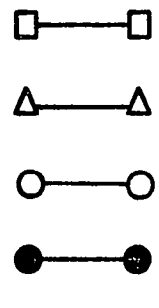

Data of Jones and Murchison (24) (normal)

First series of samples with $G_b < 10.0$ (hemispherical)

First series of samples with $G_b > 10.0$ (hemispherical)

Second and third series of samples (hemispherical)

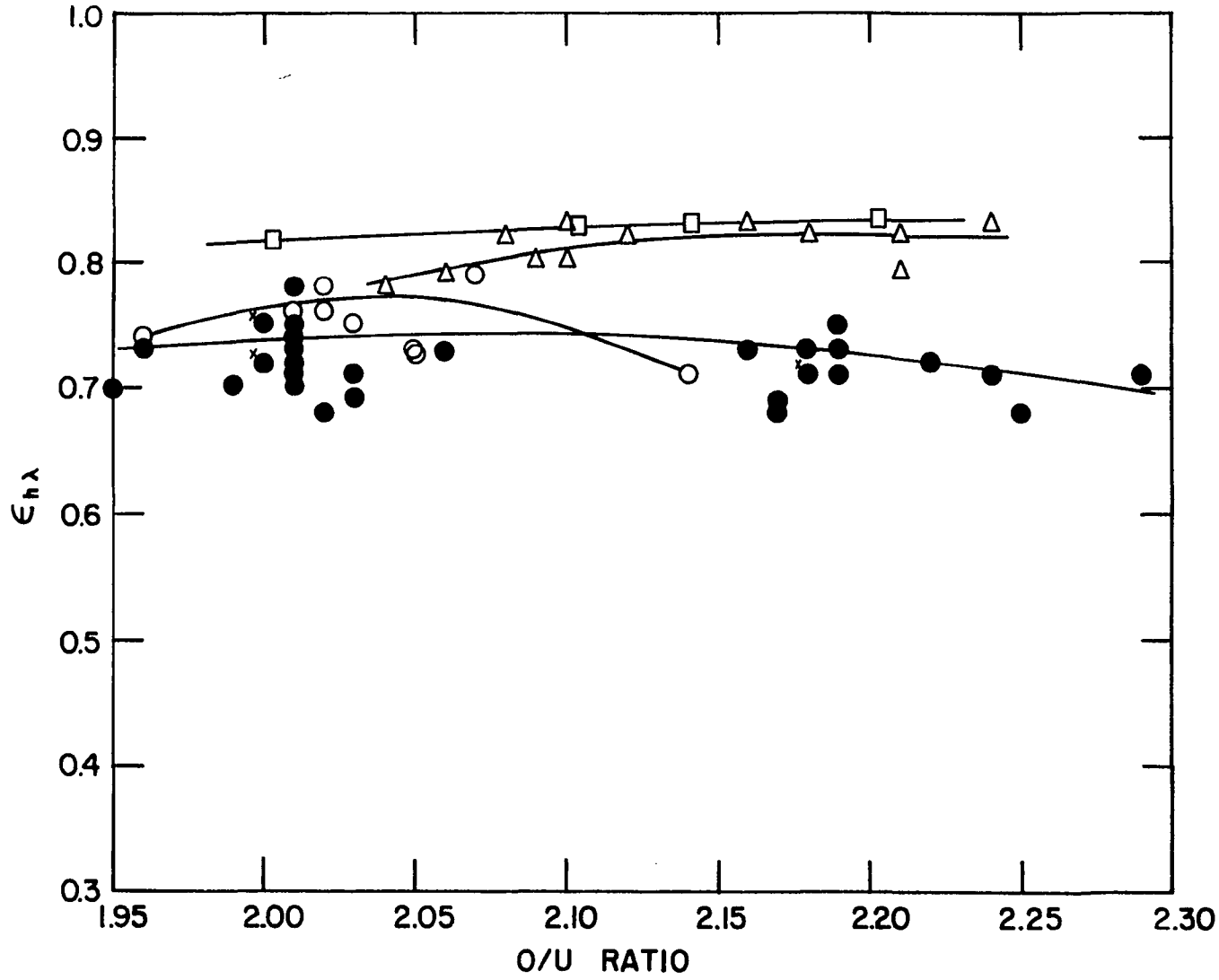
1.0
0.9
0.8
0.7
0.6
0.5
0.4
0.3
$\epsilon_{h\lambda}$
1.95
2.00
2.05
2.10
2.15
2.20
2.25
2.30
O/U RATIO

Figure 8. Emittance of uranium oxides at 0.656μ with one screen in the optical path without regard to density

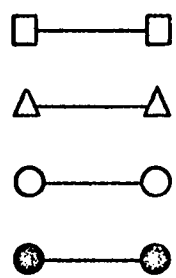

$T < 1955^{o}K$

$1955^{o}K < T < 2058^{o}K$

$2058^{o}K < T < 2213^{o}K$

$2213^{o}K < T$

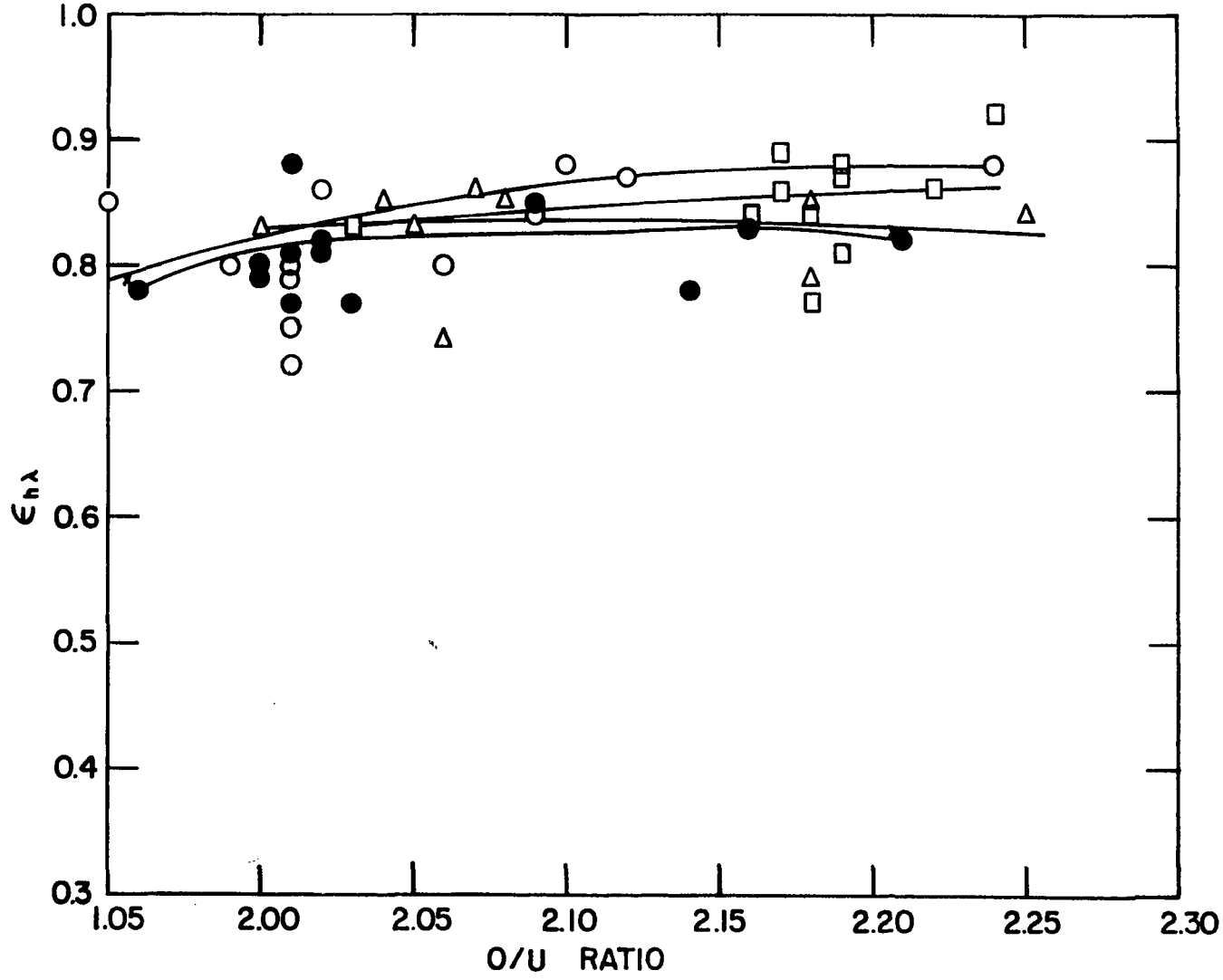
1.0
0.9
0.8
0.7
0.6
0.5
0.4
0.3
$\epsilon_{h\lambda}$
1.05
2.00
2.05
2.10
2.15
2.20
2.25
2.30
O/U RATIO

Figure 9. Emittance of uranium oxides at 0.656μ with no screens in the optical path without regard to density

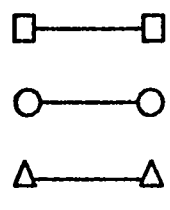

$T < 2162^{o}K$

$2162^{o}K < T < 2315^{o}K$

$2315^{o}K < T$

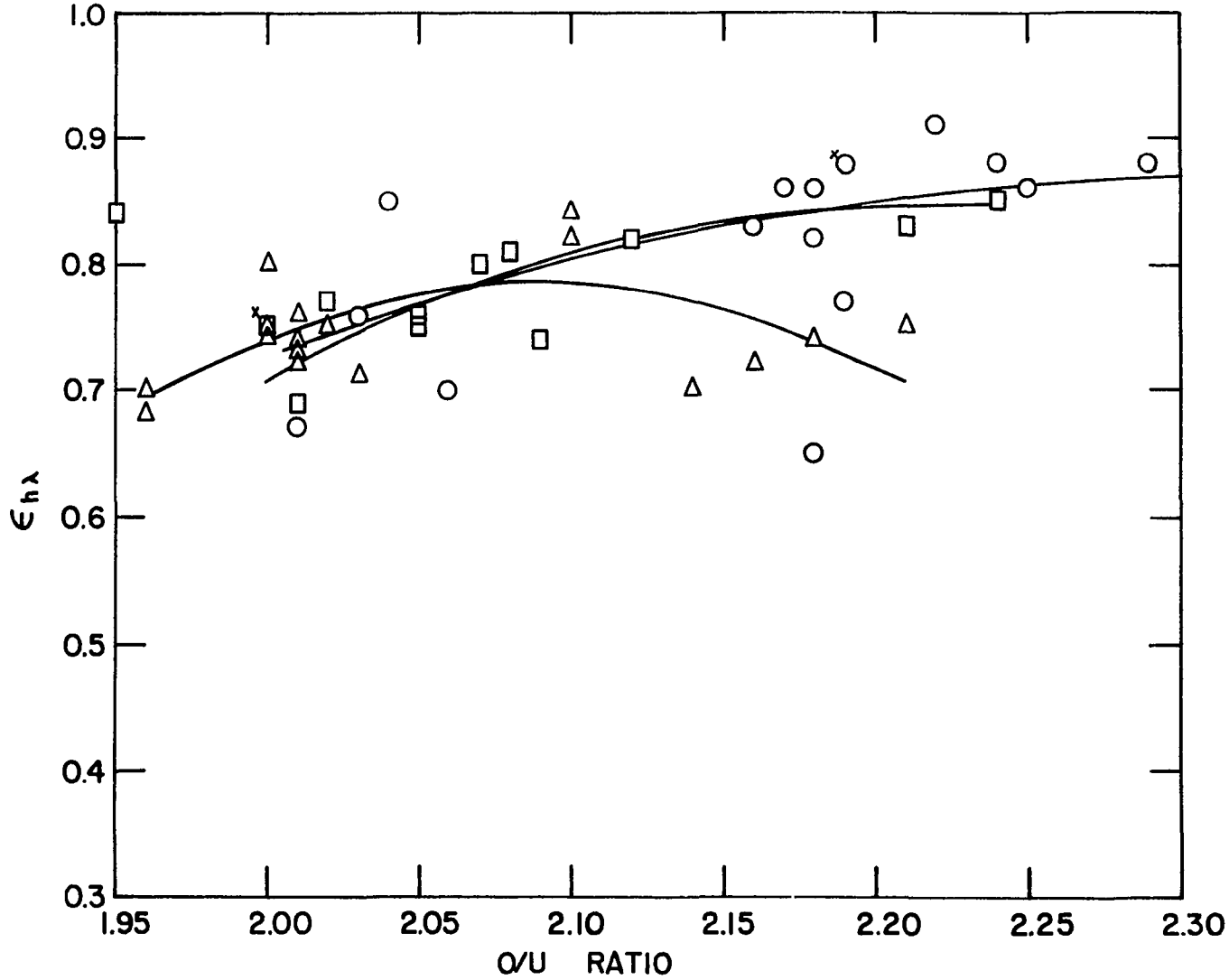
1.0
0.9
0.8
0.7
0.6
0.5
0.4
0.3
$\epsilon_{h\lambda}$
1.95
2.00
2.05
2.10
2.15
2.20
2.25
2.30
O/U RATIO

Figure 10. Emittance of uranium oxides at 0.70μ without regard to density

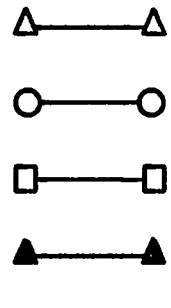

Four screens in the optical path (hemispherical)

One screen in the optical path (hemispherical)

Zero screens in the optical path (hemispherical)

Data of Jones and Murchison (24) (normal)

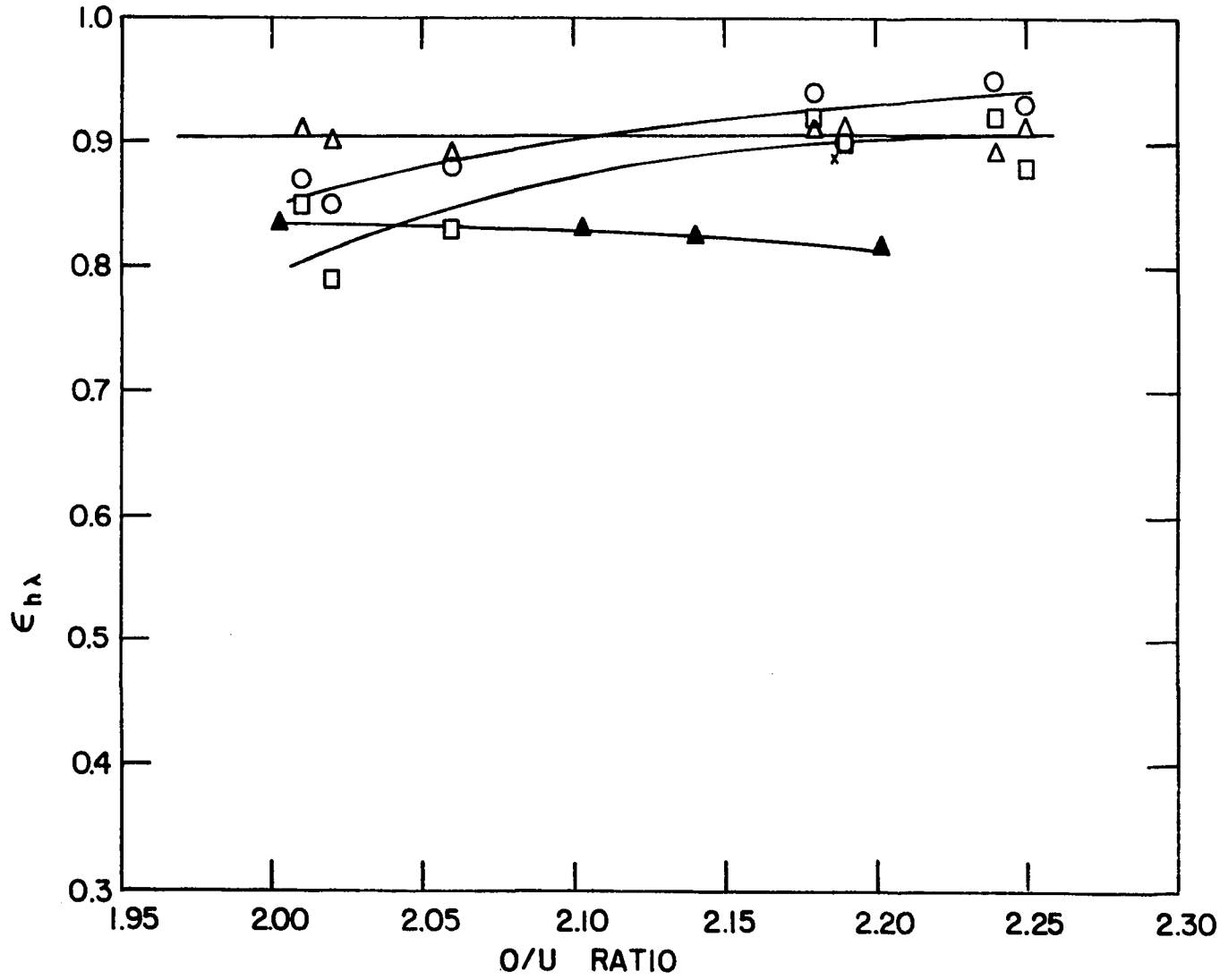
1.0
0.9
0.8
0.7
0.6
0.5
0.4
0.3
$\epsilon_{h\lambda}$
1.95
2.00
2.05
2.10
2.15
2.20
2.25
2.30
O/U RATIO

DISCUSSION

The most important single observation that can be made from these data is that the emittance of uranium oxides is not a sensitive function of temperature, density, porosity, or O/U ratio.

The emittance at high temperatures is a few per cent higher than at low temperatures. There seems to be a maximum in the emittance at high temperatures but the difference in emittance is within the scatter of the data.

The difference in emittance between the low and high temperature measurements may be due to a genuine temperature effect but could also be due to surface roughening as discussed later. These observations are in direct conflict with the work of Claudson (22) and Ehlert and Margrave (23) who found the emissivity decreased strongly with increasing temperature. If one considers the emittance of a material as a measure of the ability to absorb energy, then a defective material like uranium oxide would be unlikely to lose absorption processes at high temperature if the absorption process can be related to a defect structure. Since Bates (29) reports several absorption peaks near 0.65μ as probably related to defect structure it would seem unlikely that no defect would

be left to absorb energy at high temperature.

The density of the specimens did not seem to affect the emittance on any noticeable scale with the exception of the data taken on the first series of samples at room temperature. Since the samples with the lowest densities were very poorly sintered, slaking in water, the slight trend here is more surprising for its low degree of resolution than for its appearance at all.

The O/U ratio seemed to effect the emittance in the most consistent manner and follows the general trend found by Jones and Murchison (24) in almost every grouping. This trend is most likely related to the defect state of the material. That is, the higher the O/U ratio the more defects are available to absorb energy and consequently the higher the emittance. Since $UO_{2.00}$ absorbs energy quite well the absorption mechanism is still in operation at the stoichiometric composition. Thermal vibrations of the ions or defects in the oxygen lattice would seem the most likely mechanisms to absorb energy at the stoichiometric composition since these defects must always be present.

The increased emittance at 0.70μ is hard to explain in terms of the absorption spectra of Bates (29) but tends to

agree with the measurements of Jones and Murchison (24). This wave length is a little high to be right on the room temperature absorption edge. However, if the absorption edge is made up of several peaks as indicated (29) then emittance data at small wave length intervals might help resolve the peaks in the absorption spectra.

The room temperature emittance values have a further significance when compared to the data of Jones and Murchison (24). The magnitude of the hemispherical spectral emittance is about 92% of the normal spectral value. Thus, uranium oxides come close to obeying Lambert's cosine law, at least when integrated over a hemisphere.

It is not possible to conclude from these experiments whether the increased emittance observed at high temperatures depends on temperature, surface, or a combination of the two factors. It is generally felt that a surface must be very smooth for the emittance to be a function of the material only. However, Richmond (46) and Gordon (47) believe the surface can even be sandblasted and not affect the emittance. If the surface does not affect the emittance, the increase in emittance with temperature is real and the emittance values reported here are very close to emissivities. If the surface

alone increases the emittance at high temperatures, due to roughening by volatilization, then the emittance values are correct. In this latter case it would be nearly impossible to measure the emissivity of uranium oxides as their vapor pressure is quite high and would always tend to roughen the surface.

As has been mentioned, the emissivity of a body could be calculated from the optical constants if the optical constants were known as a function of temperature, composition, and density. Since the emittance of these oxides did not vary greatly it would seem that the optical constants are not a very sensitive function of these variables.

The errors inherent in this type of measurement have been reviewed by McMahon (40) and Wilson (39). The largest error source probably comes from measuring the furnace constant K. This value ranged from about 0.6 to 0.8 in the several calibrations. However, the emittances did not seem to vary proportionately to K but in their own manner. The drop in temperature while the shutter closes produces an error in temperature and emittance. Wilson (39) reports that the emittance should be 2-3% low due to this error, while the temperature errors may be somewhat higher. Since this study indicates

that the emittance is not a sensitive function of temperature such errors in temperature have been ignored.

The densities of the samples were increased and the porosities decreased during these measurements even though the heating time was generally less than two minutes with only a few seconds at the highest temperatures. Further, there appeared to be some reduction of the samples with the highest O/U ratios and oxidation of samples with the lowest O/U ratios. Finally, there is some doubt that the stoichiometry values are completely accurate due to the errors inherent in microbalance work. None of these errors are great enough to invalidate the general trends found in this study.

CONCLUSIONS

1. The method of Comstock as modified by McMahon has been used to measure the hemispherical spectral emittance of uranium oxides from near room temperature to about 2400°K.

2. The emittance values were determined at wave lengths of 0.656μ and 0.70μ and showed a tendency to increase with increasing wavelength contrary to what is expected from published absorption data.

3. The emittances, under all variations in temperature, O/U ratio, density, porosity, and surface finish were high. Values ranged from about 0.70 to 0.88.

4. The emittance does not decrease with temperature as previously reported.

5. The slight decrease in emittance with decreasing O/U ratio reported at room temperature may also hold at high temperatures.

6. The high absorptance and emittance of uranium oxides is probably related to the absorption edge in uranium oxides.

LITERATURE CITED

1. Belle, J., ed. Uranium dioxide: properties and nuclear applications. Washington, D.C., Naval Reactors, Division of Reactor Development, U.S. Atomic Energy Commission. 1961.

2. Held, P. C. Vaporization of solid UO_2. Unpublished M.S. thesis. Ames, Iowa, Library, Iowa State University of Science and Technology. 1965.

3. Cuy, E. J. Ionic sizes and their relationship to crystal structure type, solid solution and double salt formation and the stabilities of hydrates and ammoniates. American Chemical Society Journal 49: 201-215. 1927.

4. Anderson, J. S. Travaux récents sur la chimie des oxydes d'uranium. Société Chimique de France Bulletin 20: 781-788. 1953.

5. Pério, P. Considérations sur les oxydes d'uranium compris entre UO_2 et U_3O_8. Société chimique de France Bulletin 20: 840-841. 1953.

6. Hoekstra, H. R., Santoro, A., and Siegel, S. The low temperature oxidation of UO_2 and U_4O_9. Journal of Inorganic and Nuclear Chemistry 18: 166-178. 1961.

7. Pério, P. L'oxydation de UO_2 à basse température. Société Chimique de France Bulletin 20: 256-263. 1953.

8. Grønvold, F. High temperature x-ray study of uranium oxides in the UO_2-U_3O_8 region. Journal of Inorganic and Nuclear Chemistry 1: 357-370. 1955.

9. Willardson, R. K., Moody, J. W., and Goering, H. L. The electrical properties of uranium oxides. Journal of Inorganic and Nuclear Chemistry 6: 19-33. 1958.

10. Roberts, L. E. J. and Walter, A. J. Equilibrium pressures and phase relations in the uranium oxide system. Journal of Inorganic and Nuclear Chemistry 22: 213-229. 1961.

11. Belbeoch, B., Piekarski, C., and Pério, P. Structure de U_4O_9. Acta Crystallographica 14: 837-843. 1961.

12. Willis, B. T. M. Point defects in uranium oxides. British Ceramic Society Proceedings 1, No. 1: 9-19. 1964.

13. Willis, B. T. M. Structures of UO_2, UO_{2+x}, and U_4O_9 by neutron diffraction. Journal de Physique 25: 431-439. 1964.

14. Thorn, R. J. and Winslow, G. H. Oxygen self diffusion in uranium dioxide. Journal of Chemical Physics 44: 2822-2826. 1966.

15. Thorn, R. J. and Winslow, G. H. Nonstoichiometry in uranium oxides. Journal of Chemical Physics 44: 2632-2643. 1966.

16. Alberman, K. B. and Anderson, J. S. The oxides of uranium. Chemical Society (London) Journal, Supplement and Index 1949: S303-S311. 1949.

17. Anderson, J. S., Roberts, L. E. J., and Harper, E. A. The oxidation of uranium dioxide. Chemical Society (London) Journal 1955: 3946-3959. 1955.

18. Pério, P. Contribution to the crystallography of the uranium-oxygen system (translated title). France. Commissariat à l'Énergie Atomique Report CEA-363 [Paris]. 1955.

19. Aronson, S., Roof, R. B., and Belle, J. Kinetic study of the oxidation of uranium dioxide. Journal of Chemical Physics 27: 137-144. 1957.

20. Smith, T. Kinetics and mechanism of the oxidation of uranium dioxide and uranium dioxide plus fissia sintered pellets. U.S. Atomic Energy Commission Report NAA-SR-4677 [North American Aviation Inc., Downey, Calif.]. 1960.

21. Willis, B. T. M., Lambe, K. A., and Valentine, T. M. A neutron diffraction study of the thermal motions of

the atoms in urania and thoria. Gt. Brit. Atomic Energy Research Establishment Report AERE-R-4001 [Harwell, Berks, England]. 1962.

22. Claudson, T. T. Emissivity data for uranium dioxide. U.S. Atomic Energy Commission Report HW-55414 [General Electric Co. Hanford Atomic Products Operation, Richland, Wash.]. 1958. Original not available; cited in Belle, J., ed. Uranium dioxide: properties and nuclear applications. pp. 196-197. Washington, D.C., Naval Reactors, Division of Reactor Development, U.S. Atomic Energy Commission. 1961.

23. Ehlert, T. C. and Margrave, J. L. Melting point and spectral emissivity of uranium dioxide. American Ceramic Society Journal 41: 330. 1958.

24. Jones, J. M. and Murchison, D. G. Optical properties of uranium oxides. Nature 205: 663-665. 1965.

25. Ellis, W. P. Criterion of surface roughness applied to reflection by fluoride interference films on uranium dioxide: refractive index of uranium dioxide. Optical Society of America Journal 54: 265-266. 1964.

26. Ackermann, R. J., Thorn, R. J., and Winslow, G. H. Visible and ultraviolet absorption properties of uranium dioxide films. Optical Society of America Journal 49: 1107-1112. 1959.

27. Companion, A. and Winslow, G. H. Diffuse reflectance measurements on bulk uranium dioxide. Optical Society of America Journal 50: 1043-1045. 1960.

28. Gruen, D. M. Absorption spectra and electrical conductivities of UO_2-ThO_2 solid solutions. American Chemical Society Journal 76: 2117-2120. 1954.

29. Bates, J. L. Visible and infrared absorption spectra of uranium dioxide. Nuclear Science and Engineering 21: 26-29. 1965.

30. Harrison, T. R. Radiation pyrometry and its underlying principles of radiant heat transfer. New York, New York, John Wiley and Sons, Inc. 1960.

31. Kröeger, F. A. Search for a defect model for UO_2. Zeitschrift für Physikalische Chemie Neue Folge 49: 178-197. 1966.

32. Wolf, R. A. The electrical conductivity and thermoelectric power of uranium dioxide. U.S. Atomic Energy Commission Report WAPD-270 [Westinghouse Electric Corp. Atomic Power Div., Pittsburg]. 1963.

33. Bates, J. L., Hinman, C. A., and Kawada, T. Electrical conductivity of UO_2. Part I. Single crystals. U.S. Atomic Energy Commission Report BNWL-296 (Pt. 1) [Battelle-Northwest, Richland, Wash.]. 1966.

34. Kubela, P. and Munk, F. Ein Betrag zur Optic der Farbanstriche. Zeitschrift für Technische Physik 12: 593-601. 1931.

35. Richmond, J. C. Relation of emittance to other optical properties. National Bureau of Standards Journal of Research 67C: 217-226. 1963.

36. Folweiler, R. C. and Mallio, J. Thermal radiation characteristics of transparent semi-transparent and translucent materials under non-isothermal conditions. U.S. Department of Commerce, Office of Technical Services, Technical Documentary Report ASD-TDR-62-719, Part 2. 1964.

37. Laszlo, T. S. Temperature and flux versus geometrical perfection. Journal of Solar Energy Science and Technology 1, Nos. 2 & 3: 78-83. 1957.

38. Comstock, D. F., Jr. A radiation technique for determining the emittance of refractory oxides. In Richmond, J. C., ed. Measurement of thermal radiation properties of solids: NASA SP 31. pp. 461-468. Washington, D.C., U.S. Government Printing Office. 1962.

39. Wilson, R. G. Hemispherical spectral emittance of ablation chars, carbon, and zirconia to 3700°K. In Katzoff, S., ed. Symposium on thermal radiation of solids: NASA SP 55. pp. 259-275. Washington, D.C., U.S. Government Printing Office. 1965.

40. McMahon, W. R. Hemispherical spectral emittance of selected rare earth oxides. Unpublished Ph.D. thesis. Ames, Iowa, Library, Iowa State University of Science and Technology. 1967.

41. Weinstein, M. A. On the validity of Kirchoff's law for a freely radiating body. American Journal of Physics 28: 123-125. 1960.

42. American Society for Testing Materials. Preparation of a magnesium oxide standard for spectral reflectivity. A.S.T.M. Designation; D 986-50, Pt. 6 of 1961: 255-227. 1961.

43. Knowles Middleton, W. E. and Sanders, C. L. The absolute spectral diffuse reflectance of magnesium oxide. Optical Society of America Journal 41: 419-424. 1951.

44. Fuhrman, N., Hower, L. D., and Holden, R. B. Low-temperature sintering of uranium dioxide. American Ceramic Society Journal 46: 114-121. 1963.

45. Aronson, S. and Belle, J. Nonstoichiometry in uranium dioxide. Journal of Chemical Physics 29: 151-158. 1958.

46. Richmond, J. C. Effect of surface roughness on emittance of nonmetals. Optical Society of America Journal 56: 253-254. 1966.

47. Gordon, A. R. Emissivity of a surface after sandblasting. High Temperature 3: 811-817. 1965.

ACKNOWLEDGEMENTS

The author would like to express his special thanks to Dr. D. R. Wilder for his encouragement and understanding during the course of this research.